



Stern- und
Planetenentstehung
Sommersemester 2020
Markus Röllig

Lecture 6: Giant Molecular Clouds



http://exp-astro.physik.uni-frankfurt.de/star_formation/index.php

VORLESUNG/LECTURE

Raum: Physik - 02.201a

dienstags, 12:00 - 14:00 Uhr

SPRECHSTUNDE:

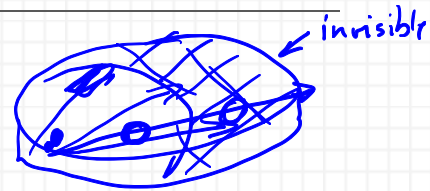
Raum: GSC, 1/34, Tel.: 47433, (roellig@ph1.uni-koeln.de)

dienstags: 14:00-16:00 Uhr

Nr.	Thema	Termin
1	Observing the cold ISM	21.04.2020
2	Observing Young Stars	28.04.2020
3	Gas Flows and Turbulence Magnetic Fields and Magnetized Turbulence	05.05.2020
4	Gravitational Instability and Collapse	12.05.2020
5	Stellar Feedback	19.05.2020
6	Giant Molecular Clouds	26.05.2020
7	Star Formation Rate at Galactic Scales	02.06.2020
8	Stellar Clustering	09.06.2020
9	Initial Mass Function – Observations and Theory	16.06.2020
10	Massive Star Formation	23.06.2020
11	Protostellar disks and outflows – observations and theory	30.06.2020
12	Protostar Formation and Evolution	07.07.2020
13	Late Stage stars and disks – planet formation	14.07.2020

6 GIANT MOLECULAR CLOUDS

In the MW and nearby galaxies we can resolve GMCs.



MW: better resolution

nearby galaxies: unbiased view (no confusion, distance ambiguity) of all GMCs



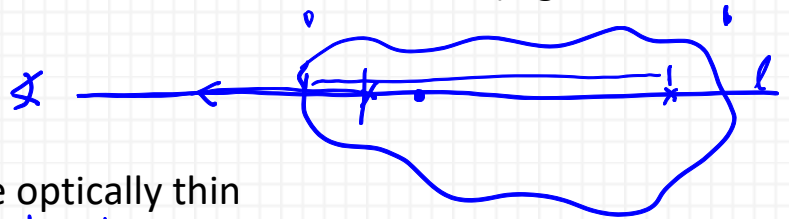
statistical inferences from nearby galaxies tested in MW.

6.1 MOLECULAR CLOUD MASSES

6.1.1 Mass Measurements

Mass of molecular cloud: most basic and most difficult to measure.

Most commonly: mass derived from molecular line emission (e.g.: ^{12}CO , ^{13}CO , HCN)



OPTICALLY THIN LINES

^{13}CO simplest: generally lines are optically thin

Local thermal equil.

For emitting molecules in LTE at temperature T:

$$I_\nu = (1 - e^{-\tau_\nu}) B_\nu(T)$$

$B_\nu(T)$: Planck function

thick $\tau_\nu \gg 1: e^{-\tau_\nu} \rightarrow 0,$

$I_\nu \rightarrow B_\nu(T)$ thus

$$I_\nu \propto T$$

*Rayleigh
Jeans*

thin $\tau_\nu \ll 1: e^{-\tau_\nu} \rightarrow 1 - \tau_\nu,$

$I_\nu \rightarrow \tau_\nu B_\nu(T)$ thus

$$I_\nu \propto \tau_\nu$$

$$\tau \sim N_{^{12}\text{CO}}$$

$$\tau = \int \alpha \rho \, dx$$

$$\alpha = n \cdot \sigma$$

e.g.: ^{12}CO is typically optically thick

$$\Rightarrow I_\nu(^{12}\text{CO}) = B_\nu(T)$$

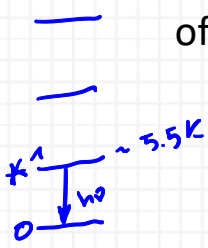
gives temperature T

then ^{13}CO , which is typically optically thin, assuming the same temperature T

$$\Rightarrow I_\nu(^{13}\text{CO}) = (1 - e^{-\tau_\nu(^{13}\text{CO})}) B_\nu(T)$$

gives opt. depth $\tau_\nu(^{13}\text{CO})$

If N_{13CO} is the column density of ^{13}CO , then in LTE, the column densities of atoms in level 0 and 1 state are:



$$n_0 = \frac{N_{13CO}}{Z}$$

$$n_1 = e^{-T/T_1} \frac{N_{13CO}}{Z}$$

Z: partition function (f(T))
 $T_1=5.3K$, energy of J=1 level

$B_{0,1}$ 0 \rightarrow 1

opacity to line absorption:

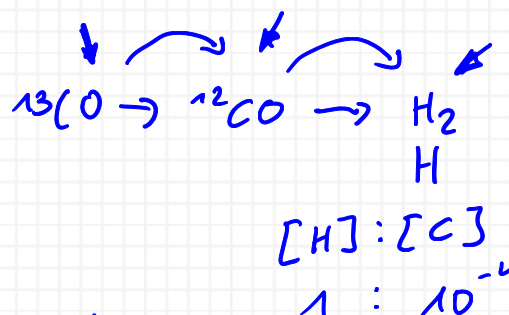
$$\kappa_\nu = \frac{h\nu}{4\pi} (n_0 B_{01} - n_1 B_{10}) \phi(\nu)$$

B_{01}, B_{10} : Einstein coeff. for spontaneous absorption and stimulated emission

$\phi(\nu)$: line profile \rightarrow measure the line shape

$$\tau_\nu = \frac{h\nu}{4\pi} (N_0 B_{01} - N_1 B_{10}) \phi(\nu)$$

N_{13CO} only unknown!



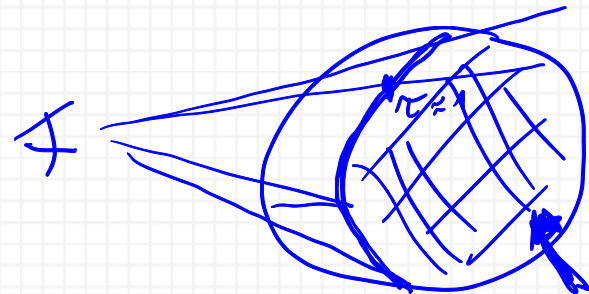
Problems:

- assume 12-13 CO ratio 66:1
- assume CO-H ratio
- ^{12}CO and ^{13}CO have same temperature
- LTE assumption (^{13}CO sub-thermal?)
- ^{13}CO line probably too faint for extragalactic observations

OPTICALLY THICK LINES

optically thick lines are bright

- good for distant objects
- bad for mass determination



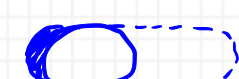
Common approach: define an "X-factor" (scaling between the observed frequency-integrated intensity and the total column density of gas)

$$X_{CO} = \frac{N}{I_{CO}} \approx 2 - 3 \times 10^{20} \text{ cm}^{-2} \text{ K}^{-1} \text{ km}^{-1} \text{ s}$$

N: true column density (H_2 molecules per cm^2)

surprise: universal X-factor

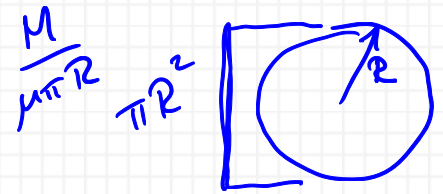
$1 \text{ K km s}^{-1} \Rightarrow N_{H_2} \approx 2.3 \times 10^{20} \text{ cm}^{-2}$



If cloud is optically thick, why should the I_ν measure the whole cloud mass?

mean column density: $N = M / (\mu \pi R^2)$

$\mu = 3.9 \times 10^{-24}$ g (mass per H_2 molecule)



total integrated intensity:

$$\int I_\nu d\nu = \int (1 - e^{-\tau_\nu}) B_\nu(T) d\nu$$

Virial equilibrium: $\mathcal{T} = \mathcal{W}/2$, so that $\dot{I} = 0$

$$\mathcal{W} = aGM^2/R$$

a: constant (order unity) describing the geometry

uniform sphere $\Rightarrow a = 3/5$

$$\mathcal{T} = \left(\frac{3}{2}\right) M \sigma_{1D}^2$$

σ_{1D} : 1-D velocity dispersion (thermal+non-thermal)

virial ratio: $\alpha_{vir} = \frac{5\sigma_{1D}^2 R}{GM}$ for uniform sphere $\alpha_{vir} = \frac{2\mathcal{T}}{\mathcal{W}} = 1$

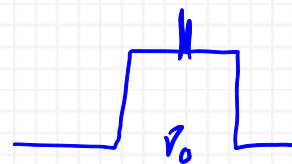
in general: $\alpha_{vir} \approx 1$ in any object supported primarily by turbulent motion.

$$\sigma_{1D} = \sqrt{\left(\frac{\alpha_{vir}}{5}\right) \frac{GM}{R}}$$



remember that $\int I_\nu d\nu = \int (1 - e^{-\tau_\nu}) B_\nu(T) d\nu$

optical depth at line center $\tau_{\nu_0} \gg 1$ and Gaussian line profile:



$$\tau_\nu = \tau_{\nu_0} \exp\left[-\frac{(\nu - \nu_0)^2}{2(\nu_0 \sigma_{1D}/c)^2}\right]$$

so we expect: $I_\nu = f(\sigma_{1D})$

Example: step function $\tau_\nu(\nu_0) = \infty$ and $\tau_\nu(|\nu - \nu_0| > \Delta\nu) \rightarrow 0$

from $\tau_\nu = 1$ (that is \sim where the transition from center to wing takes place) follows

$$\Delta v = |v - v_0| = v_0 \sqrt{2 \ln \tau_{v_0} \frac{\sigma_{1D}}{c}} \quad \tau_{v_0} = \tau(v=v_0)$$

in velocity (Doppler shift):

$$\Delta v = \sqrt{2 \ln \tau_{v_0} \sigma_{1D}}$$

The corresponding brightness temperatures then are:

$$T_{B,v} = \begin{cases} T, & |v - v_0| < \Delta v \\ 0, & |v - v_0| > \Delta v \end{cases}$$

then

$$I_{CO} = \int T_{B,v} dv = 2T_B \Delta v = \sqrt{8 \ln \tau_{v_0} \sigma_{1D} T} \propto \sigma_{1D}$$

$\sqrt{\ln \tau_{v_0}}$: negligible

Thus, the velocity-integrated brightness temperature is simply proportional to σ_{1D}

Therefore:

$$\begin{aligned} X [cm^{-2} (K km s^{-1})^{-1}] &= \frac{M}{\mu \pi R^2 I_{CO}} \\ &= \frac{10^5 (8 \ln \tau_{v_0})^{-\frac{1}{2}} M}{T \mu \pi \sigma_{1D} R^2} \\ &= \frac{10^5 (8 \ln \tau_{v_0})^{-\frac{1}{2}}}{T \mu \pi} \sqrt{\frac{5n}{6\pi \alpha_{vir} G}} \end{aligned}$$

with $n = \frac{3M}{4\pi R^3}$, (factor 10^5 because I_{CO} is in $km s^{-1}$ instead of $cm s^{-1}$)

$$\text{Example: } n = 100 cm^{-3}, T = 10K, \alpha_{vir} = 1, \tau_{v_0} = 100 \Rightarrow X = 5 \times 10^{19} cm^{-2} (K km s^{-1})^{-1}$$

Very simplified! Observations show:

from γ ray emission (interaction between CR and ISM, basically no attenuation) $X \approx 2 \times 10^{20} cm^{-2} (K km s^{-1})^{-1}$ (Strong & Mattox (1996))

from dust grains:

$$X \approx 2 \times 10^{20} \text{ cm}^{-2} (\text{K km s}^{-1})^{-1} \text{ (Dame et al (2001))}$$

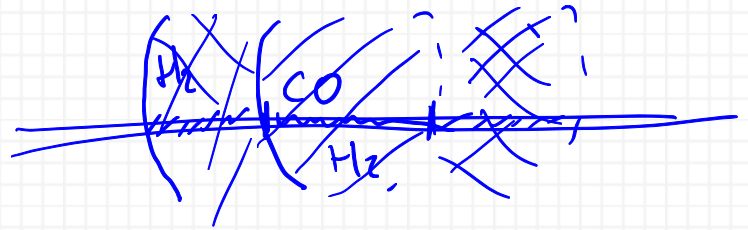
$$X \approx 4 \times 10^{20} \text{ cm}^{-2} (\text{K km s}^{-1})^{-1} \text{ (Draine et al (2007))}$$

Under Milky Way conditions, accurate to within a factor ~ 2 .

Turning the analysis around shows that GMC are probably not too far from virial balance.

Problems: assumption that CO and H₂ are tightly correlated (might break down in low metallicity cases)

also: CO-dark H₂ gas



6.1.2 Mass Distribution

In the MW and nearby galaxies, the molecular cloud mass distribution is fit by a truncated power-law:

$$\frac{dN}{dM} = \begin{cases} \mathcal{N}_u \left(\frac{M_u}{M}\right)^\gamma, & M \leq M_u \\ 0, & M > M_u \end{cases}$$

$$\gamma < 0$$

total GMC mass in some mass range

$$\int_{M_l}^{M_u} (dN/dM) M dM \sim M^{2+\gamma}$$

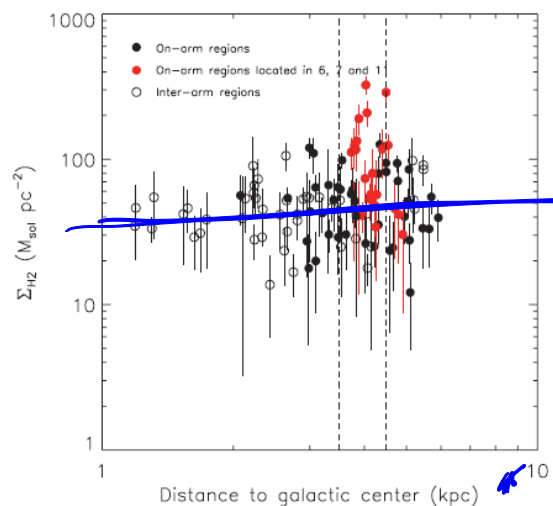
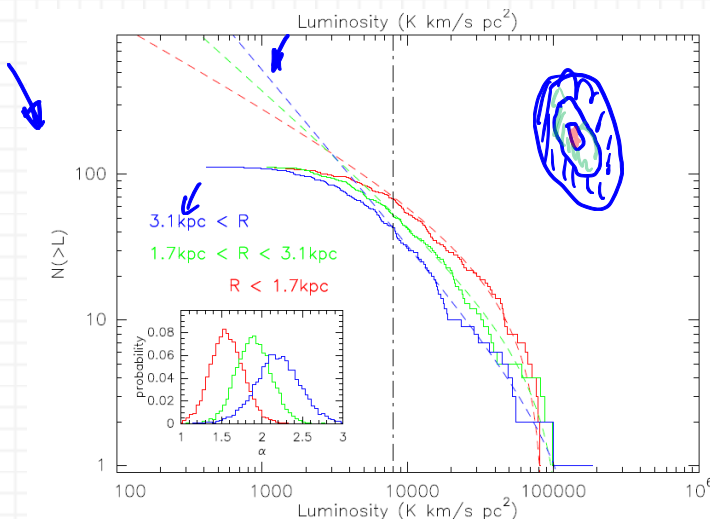


Abbildung 1 Left: Mass spectrum in M33 (Gratier et al. (2011)), Right: GMC surface density in NGC 6946 (Rebolledo et al. (2012))

$N_u, M_u,$ and γ depend on the region in the galaxies

- inner, H₂-rich parts of galaxies $\gamma = -2 \dots -1.5$
- outer parts of galaxies, metal-poor dwarf galaxies $\gamma = -2 \dots -2.5$

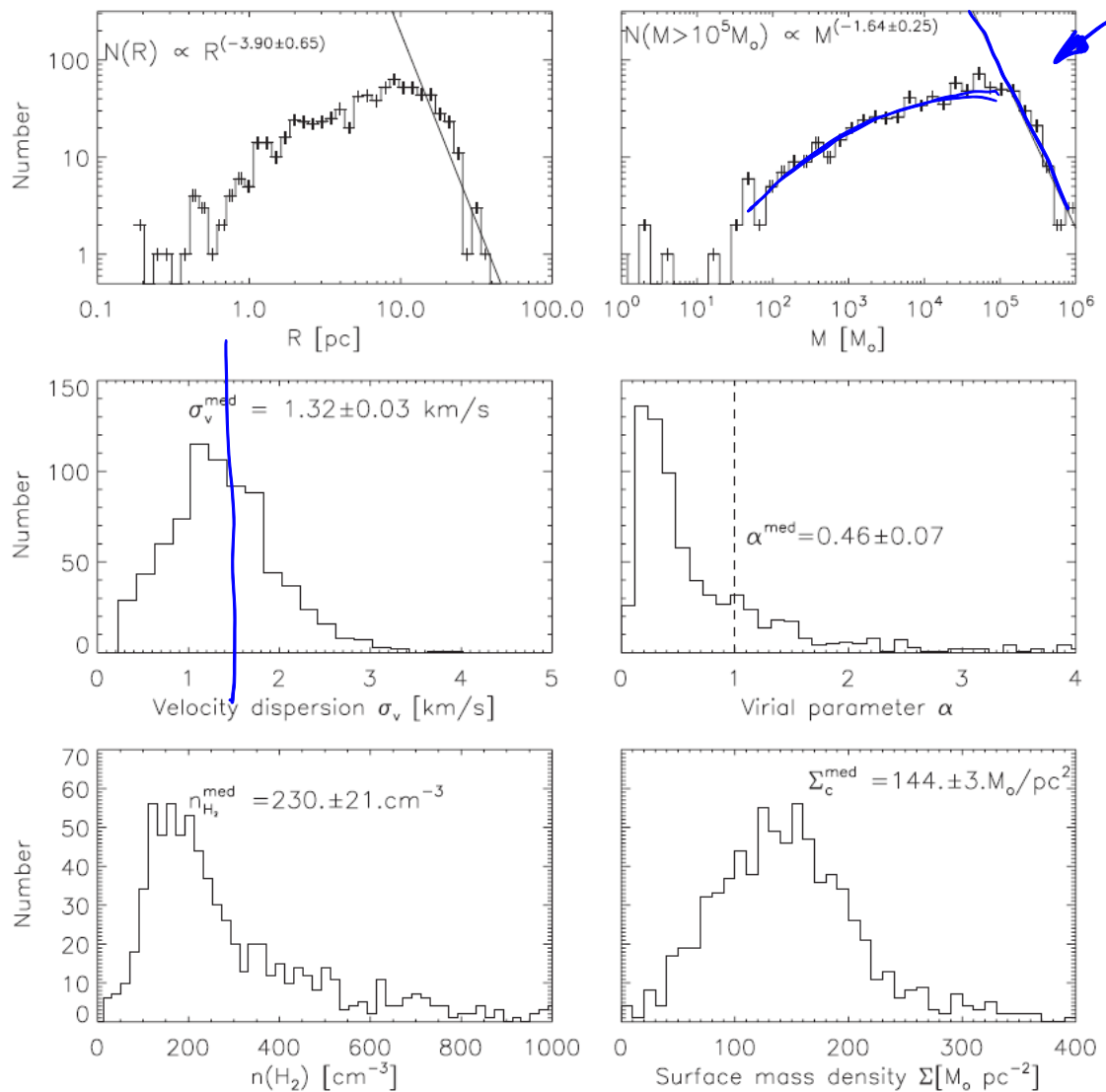


Figure 3. Histograms of the physical properties of molecular clouds. In the top two panels, the solid line indicates the best fit to the radius and mass spectra.

Abbildung 2(Roman-Duval et al. 2010)

Since most gas is found in regions with $\gamma > -2$, most of the gas in large clouds rather than small ones.

6.2 SCALING RELATIONS

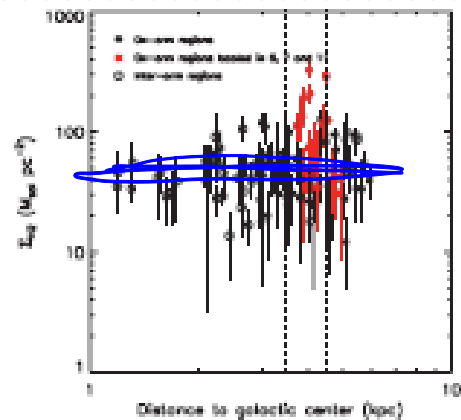
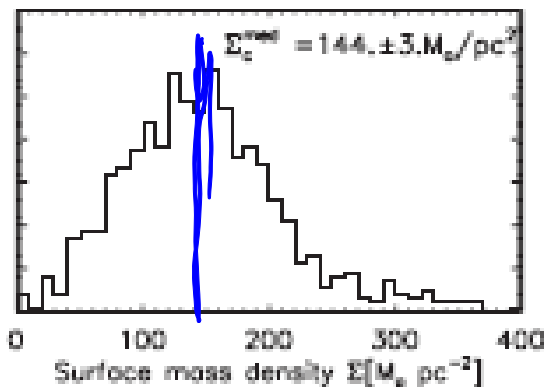
How do large-scale properties of GMCs scale with their mass?

Larson (1981) Relations:

- molecular clouds have a characteristic surface density of $\sim 100 M_{\odot} \text{pc}^{-2}$
 (LMC $\sim 50 M_{\odot} \text{pc}^{-2}$, M51 $\sim 200 M_{\odot} \text{pc}^{-2}$)
 implications for density:

$$n = \frac{3M}{4\pi R^3 \mu} = \left(\frac{3\pi^{\frac{1}{2}}}{3\mu} \right) \sqrt{\frac{\Sigma^3}{M}} = 23 \Sigma_2^{\frac{3}{2}} M_6^{-\frac{1}{2}} \text{cm}^{-3}$$

$$\Sigma_2 = \Sigma / (100 M_{\odot} \text{pc}^{-2}), \text{ and } M_6 = M / 10^6 M_{\odot}, \mu = 3.9 \times 10^{-24} \text{g}$$



Two measurements of GMC surface densities (left: MW, right: NGC6946)

- GMCs obey a linewidth-size relation

- Solomon et al (1997) find in the MW

$$\sigma = (0.72 \pm 0.07) R_{\text{pc}}^{0.5 \pm 0.05} \text{km s}^{-1}$$

- Bolatto et al. (2008) find in external galaxies:

$$\sigma = 0.44_{-0.13}^{+0.18} R_{\text{pc}}^{0.60 \pm 0.10} \text{km s}^{-1}$$

- within individual MCs in the MW Heyer & Brunt (2004) finds:

$$\sigma = 0.9 L_{\text{pc}}^{0.56 \pm 0.02} \text{km s}^{-1}$$

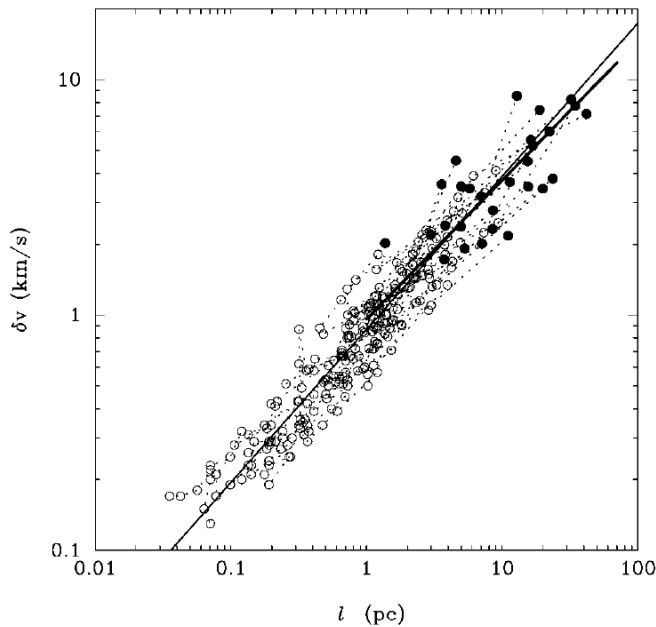


Abbildung 3 Measured correlation between GMC linewidth and size scale for MW clouds (Heyer & Brunt (2004))

- GMCs have $\alpha_{vir} \approx 1$

Larson's three laws are not independent.

We write $\sigma = \sigma_{pc} R_{pc}^{1/2}$ |

$$\alpha_{vir} = \frac{5\sigma^2 R}{GM} = \left(\frac{5}{\pi \text{ pc}}\right) \frac{\sigma_{pc}^2}{G\Sigma} = 3.7 \left(\frac{\sigma_{pc}}{1 \text{ km s}^{-1}}\right)^2 \left(\frac{100 M_{\odot} \text{ pc}^{-2}}{\Sigma}\right)$$

This implies a pressure in GMCs:

$$P = \bar{p}\sigma^2 = \frac{3\Sigma\sigma_{pc}^2}{4 \text{ pc}} \Rightarrow \frac{P}{k_B} \approx 3 \times 10^5 \text{ K cm}^{-3}$$

This is larger than typical MW values in the disk $\sim 10^4 \text{ K cm}^{-3}$

n · T
n = 10⁴ cm⁻³
T ≈ 50
P

6.3 MOLECULAR CLOUD TIMESCALES

Crossing time: characteristic time a signal needs to cross a cloud

$$t_{cr} = \frac{R}{\sigma} = \frac{0.95}{\sqrt{\alpha_{vir} G}} \left(\frac{M}{\Sigma^3} \right)^{1/4} = 14 \alpha_{vir}^{-1/2} M_6^{1/4} \Sigma_2^{-3/4} \text{ Myr}$$

Free-fall time: time required for gravitational collapse without support

$$t_{ff} = \sqrt{\frac{3\pi}{32G\rho}} = \frac{\pi^{1/4}}{\sqrt{8\pi}} \left(\frac{M}{\Sigma^3} \right)^{1/4} = 7.0 M_6^{1/4} \Sigma_2^{-3/4} \text{ Myr}$$

If $\alpha_{vir} \approx 1$, then $t_{ff} = \frac{1}{2} t_{cr} \approx 10 \text{ Myr}$

6.3.1 Depletion Time

Rate at which stars form – time to turn all gas into stars: depletion time

$$t_{dep} = M_{gas} / \dot{M}_*$$

Or for extragalactic objects (where we measure surface quantities)

$$t_{dep} = \Sigma_{gas} / \dot{\Sigma}_*$$

Difficulties:

- initial mass of a star forming cloud difficult to measure because stars disrupt the cloud
- large statistics helps

Zuckerman & Evans (1974) estimated the depletion time for the MW:

8.5 kpc

- inside solar circle the MW contains $\sim 10^9 M_{\odot}$ of molecular gas
- the star formation rate in the MW is $\sim 1 M_{\odot} \text{yr}^{-1}$

$$\Rightarrow t_{dep} = 1 \text{Gyr}$$

LONG! (10 times the crossing time!). Critical constraint for all theories.

$$\epsilon_{ff} = t_{ff}/t_{dep} \sim 1\%$$

Fraction of GMCs mass that is converted into stars per free fall time

Surveys of local galaxies find typically $t_{dep} = 2 \text{Gyr}$.

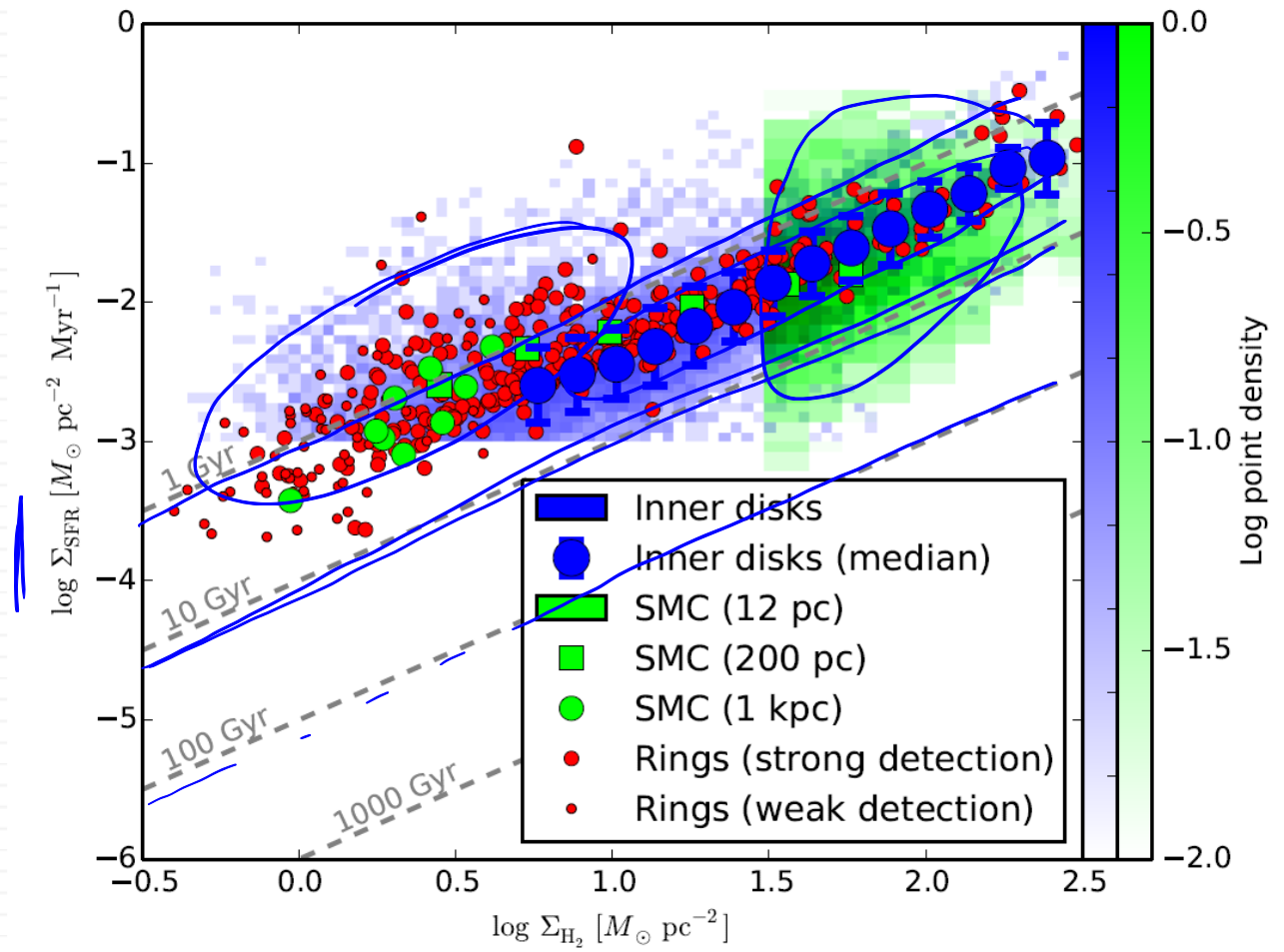


Abbildung 4 Surface density of star formation versus surface density of gas (Krumholz, 2014). Blue pixels show the distribution of pixels in the inner parts of nearby galaxies, resolved at ~ 750 pc scales Leroy et al. (2013), while green pixels show the SMC resolved at 12 pc scales Bolatto et al. (2011); other green and blue points show various averages of the pixels. Red points show azimuthal rings in outer galaxies Schrubba et al. (2011), in which CO emission can be detected only by stacking all the pixels in a ring. Gray lines show lines of constant depletion time t_{dep} .

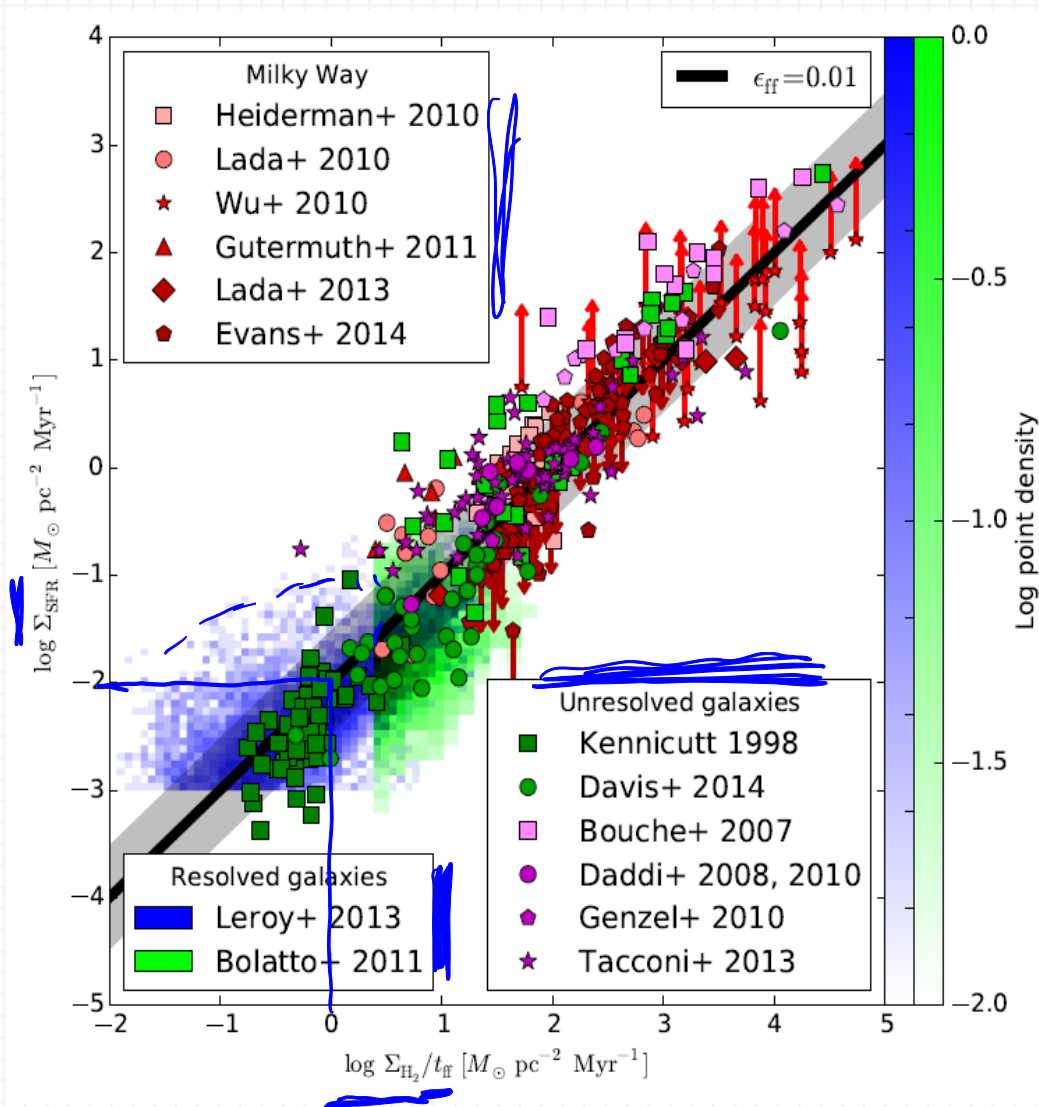


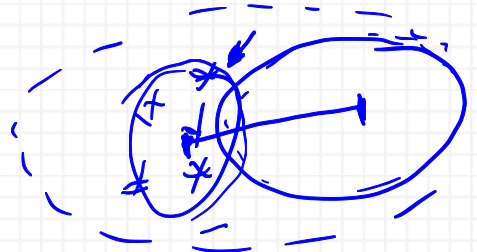
Abbildung 5 Surface density of star formation versus surface density of gas normalized by free-fall time (Krumholz, 2014). Blue and green pixels are the same as in Figure 8.5, while points represent measurements of marginally resolved galaxies (1 beam per galaxy). Points are color-coded: green indicates local galaxies, purple indicates high-z galaxies, and red indicates individual Milky Way clouds. The thick black line

6.3.2 Lifetime

How long does an individual GMC survive?

Difficulties:

- consistency in what is a GMC
- in how you estimate lifetime (t_{ff} depends e.g. on density)



Example: Kawamura et al. 2009, GMCs in the LMC

- catalogued all MCs, HII regions and all star clusters (Fukui et al. 2009)

- determined star cluster age by comparison with HR diagram MS break-off
- compute the minimum projected distance between each star cluster or HII region and the nearest GMC.

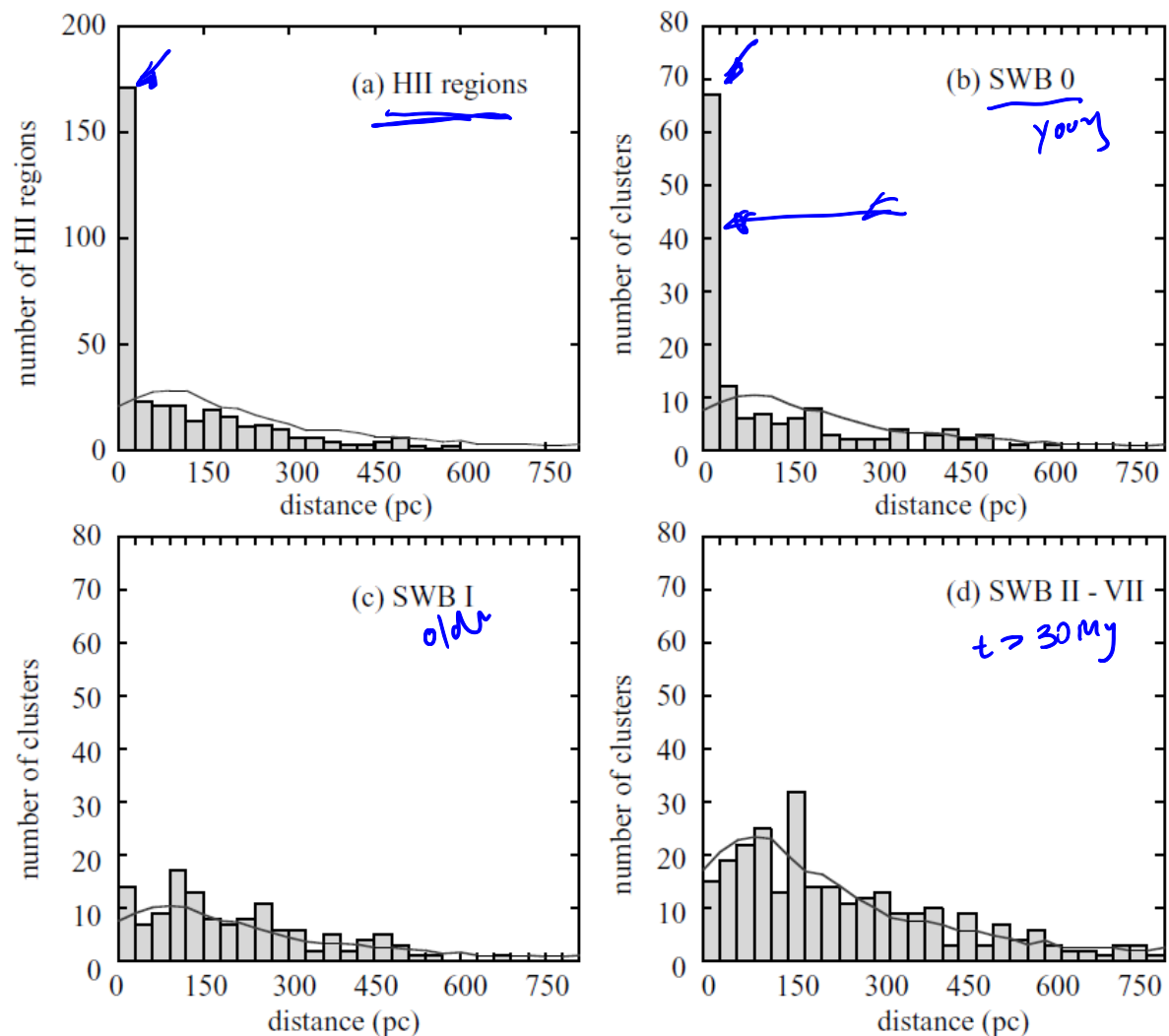


Abbildung 6 Frequency distribution of the projected distances of (a) the HII regions, (b) SWB 0 clusters ($\tau \lesssim 10 \text{ Myr}$), (c) SWB I clusters ($10 \text{ Myr} \lesssim \tau \lesssim 30 \text{ Myr}$) and SWB type II to VII clusters ($30 \text{ Myr} \lesssim \tau$, Bica et al. 1996) from the nearest molecular cloud, respectively. Lines show the frequency distribution of the distance when the HII regions and clusters are distributed randomly.

Excess of HII regions and cluster in the class SWB0 (ages $\leq 10 \text{ Myr}$) at small separations from GMCs.

\Rightarrow physical association between GMCs and those clusters and HII regions (they are near their parent cloud)

Estimate the GMC lifetimes:

$\Rightarrow \sim 60\%$ of the SWB0 cluster are in the excess spike

⇒ therefore they spend on average 60% of their 10 Myr lifetime close to the GMC

⇒ the phase of a GMC where it has a visible nearby cluster is ~6Myr

Only a minority of GMCs have nearby cluster (39), 88 are associated with HII regions and 44 are associated with neither.

⇒ assume we observe the GMCs at a random stage of their lifetimes

⇒ the fraction of GMCs with nearby clusters represents the fraction of the total GMC lifetime for which this association lasts.

$$t_{HII} = \frac{N_{HII}}{N_{cluster}} t_{cluster}$$
$$t_{quiescent} = \frac{N_{quiescent}}{N_{cluster}} t_{cluster}$$

$t_{cluster} = 6 \text{ Myr}$, then $t_{quiescent} = 7 \text{ Myr}$, $t_{HII} = 14 \text{ Myr}$

$t_{life} = t_{starless} + t_{HII} + t_{cluster} = 27 \text{ Myr} \approx 2 - 3 t_{cr} \sim \approx 4 - 6 t_{ff}$

Tricky in the MW (clusters cease to be embedded after the cluster is ~ 2-3 Myr old)

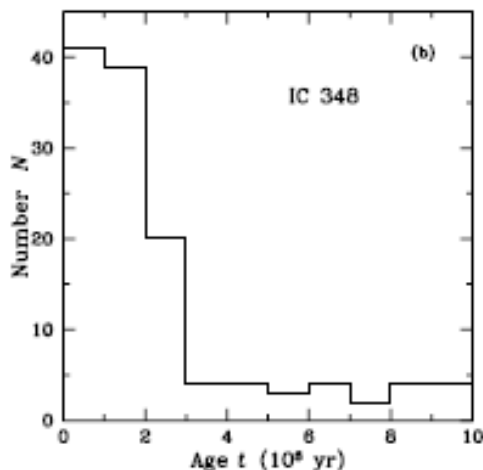


Figure 1 Histogram of inferred stellar ages in the cluster IC 348 Palla & Stahler (2000).

6.3.3 Star Formation Lag Time

Time between GMC formation and star formation onset.

Statistically, similar to previous chapter: In the LMC Kawamura et al. 2009

$$t_{\text{quiescent}} \sim 7 \text{ Myr}$$

In the solar neighborhood the ratio between clouds with and without SF is 7:1-14:1. Assuming the timescale for SF $\sim 2\text{-}3$ Myr, this implies that they have a lag time of <1 Myr .

This is smaller than the crossing time, so they are probably already starting to form stars while the GMCs are still forming.

Geometrical Measurements

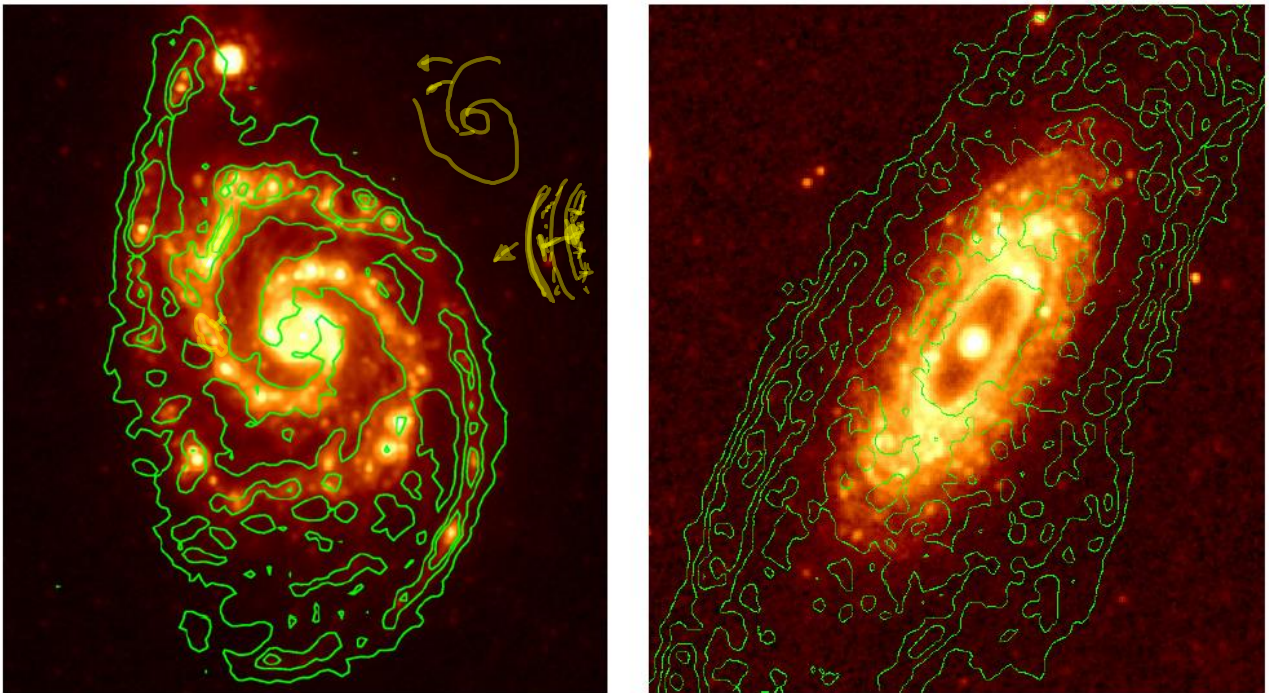


Abbildung 7 The $24\mu\text{m}$ band image is plotted in color scale for the galaxies NGC5194 (left) and NGC2841 (right); the respective HI emission map is overlaid with green contours. (Tamburro et al. 2008)

- locate spiral shocks in galaxy in HI (bulk gas) (green contours in the Fig.)
- locate a tracer of star formation (e.g. $24\mu\text{m}$ or $\text{H}\alpha$ emission)
 - the spiral shock compresses the gas and forms GMCs
 - the GMCs then start SF after some time
 - the time lag is visible in a rotation angle offset between the two because the spiral wave continues travelling.
 - the angle is proportional to the lag time (depending on the rotation speed of the galaxy)
- Tamburro et al. 2008 finds 1 – 3 Myr

